Hindawi
International Journal of Polymer Science
Volume 2019, Article ID 8453493, 7 pages
https://doi.org/10.1155/2019/8453493

Research Article

Functional Graphene Oxide Nanocarriers for Drug Delivery

Yuanfeng Ye, Xincheng Mao, Jialing Xu, Jingyang Kong, and Xiaohong Hu

School of Material Engineering, Jinling Institute of Technology, Nanjing 211169, China

Correspondence should be addressed to Xiaohong Hu; hxh@jit.edu.cn

Received 10 November 2018; Revised 23 December 2018; Accepted 31 December 2018; Published 31 January 2019

Academic Editor: Hossein Roghani-Mamaqani

The family of graphene has attracted increasing attention on account of their large specific surface area and good mechanical properties in the biomedical field. However, some characteristics like targeted delivery property and drug delivery capacity could not satisfy the need of a drug carrier. Herein, a graphene oxide (GO) nanocarrier was designed by modification of a folic acid (FA) derivative and a β-cyclodextrin (β-CD) derivative in order to improve two properties, respectively. In the first step, reactive or crosslinkable FA and aldehydic β-CD (β-CD-CHO) were designed and synthesized for further modification. In the second step, synthesized functional molecules were coupled onto GO sheets one by one to obtain the GO nanocarrier. IR spectra and XRD results were used to identify the chemical and structural information before and after modification for the GO nanocarrier. The final GO nanocarrier exhibited a typical thin wrinkled sheet morphology of the GO sheet without any influence by two functional molecules. Finally, in vitro evaluation was used to clarify the drug loading and controlling capacity of the nanocarrier as a drug delivery system. The results revealed that the GO nanocarrier had a better CPT loading capacity and showed better controllability for CPT release.

1. Introduction

The nanocarrier, a kind of submicron drug delivery system belonging to the nanoscale scope, can adjust the drug release rate, enhance the permeability of the biological membrane, change the drug distribution in vivo, and improve its efficiency through encapsulation, absorption, and even covalent crosslinking [1, 2]. In view of these advantages, nanocarriers including nanoparticles, vesicles, nanosheets, and nanocapsules have been intensively investigated in the biomedical field [1–9]. As a member of the nanocarrier, graphene oxide (GO) was also focused in the biomedical field on account of the large specific surface area, mechanical properties, and very high aspect ratio [4, 10–15]. Especially, the π-conjugated structure of GO could conjugate with a number of drug molecules either through $\pi - \pi$ stacking interaction or through chemical covalent crosslinking [4, 10–15]. However, pure GO lacks a bioactive site to support cell growth, which restricted its application in the biomedical field. Recently, researchers synthesized the carboxymethyl cellulose-modified graphene oxide (GO-CMC) complex as a drug carrier matrix, which further bonded to small molecule doxorubicin hydrochloride (DOX) by $\pi - \pi$ bond interaction and hydrogen bonding [16]. The nanocarrier exhibited a controllable drug release capacity without obvious cytotoxicity [16]. Another GO nanocarrier for the diagnosis of renal dysfunction was designed by Li et al. [10]. In the research, Ag nanoparticles (AgNPs) were synthesized on the surface of GO to promote its X-ray absorption, and simvastatin was further simultaneously introduced to eliminate the toxicity of AgNPs. Their results revealed that GO/AgNPs could enhance the signals of computed tomography (CT) in the lung, liver, and kidney of mice for a long circulation time and the presence of simvastatin ensured in vivo safety [10]. Also, the galactosylated chitosan/graphene oxide/doxorubicin (GC-GO-DOX) nanocarrier drug delivery system for cancer therapy was designed and synthesized [11]. Their results revealed that the system had obvious tumor inhibition effects [11].

Although existing methods have solved some problems of GO in the application of the biomedical field, methods and functional molecules were still needed to extend its application and solve more complex problems of organisms.

The targeted property and drug controllable property of the drug delivery system were two concerns in cancer treatment [8, 17, 18]. Therefore, functional molecules with these properties naturally become the research focus. Since folic acid can be recognized by receptors of major cells, it has been intensively investigated as a commonly used targeted molecule in the drug delivery field [19–22]. Although the targeted properties of folic acid have been verified by many researches, its application in all drug delivery systems has not been available. Hence, the exploration of folic acid in different drug delivery systems is also useful for its application and for the design of an efficient and effective drug delivery system. Herein, folic acid was functionalized onto GO in the research. Furthermore, for drug controllable properties, cyclic oligosaccharides (CDs) have exerted a profound influence on the field of drug delivery due to its capacity of holding drug molecules and controlling its release [6–9]. Among CDs, β-CD is easily available and has become a commercial pharmaceutical preparation for disease therapy. In view of these characteristics, β-CD was further introduced onto GO sheets to enhance its drug controllable property.

2. Experiment Section

2.1. Materials. Maleimide (MI), vitriol, n-hexane, folic acid (FA), β-cyclodextrin (β-CD), anhydrous dimethyl sulfoxide (DMSO), sodium periodate, glycol, acetone, and ethyl ether were purchased from Shanghai Medicine and Chemical Company, China. Trinitrobenzenesulfonic acid (TNBS), tert-butyl hydrylformate (t-BC), *N*,*N*-dicyclohexylcarbodiimide (DCC), and *N*-hydroxysuccinimide (NHS) were obtained from Shanghai Energy Chemical Limited Company. Graphene oxide (GO, purity: 99 wt%; diameter: 500 nm-5 μm thickness: 0.8-1.2 nm) was purchased from Nanjing Pioneer Nano-Tech Co. (China), which was synthesized by Hummer's method with a 99% single layer ratio. Camptothecin (CPT) was obtained from Sigma. The dialysis tube (Mw: 500-1000) was obtained from Viskase. All other reagents and solvents were of analytical grade and used as received.

2.2. Synthesis of FA-MI. Crosslinkable FA was synthesized though introduction of functional MI groups according to DCC/NHS esterification reaction. Briefly, in anhydrous DMSO, 0.4 g FA was activated by 0.4 g DCC and 0.2 g NHS for 12 h at 30°C. The resultant FA active ester was precipitated by a mixed solution (acetone : ethyl ether = 3 : 7) and further washed by ethyl ether for several times and further vacuum-dried, and FA active ester was obtained. In the next step, 0.2 g MI was dissolved in 30 mL DMSO, into which a 10 mL FA active ester DMSO solution with an equal molar ratio was added drop by drop in 1 h. After the reaction had lasted for 48 h at 40°C, the resultant solution was sealed in a dialysis bag with a cutoff molecular weight of 500 Da and dialyzed in a large amount of triple-distilled water for 3 d. Finally, FA-MI was obtained by freeze-drying and characterized by nuclear magnetic resonance hydrogen spectrum ($_1$H NMR, Bruker AV-300).

2.3. Preparation of FA Functional GO. GO was dispersed in DMSO with a final concentration of 0.1 mg/mL, into which FA-MI was added with a final concentration of 1 mg/mL. The mixture was stirred for 24 h at 60°C in the dark, which was further dialyzed with a cutoff molecular weight of 10 kDa and dried by freeze-drying. The product was characterized by infrared spectroscopy (IR, Nicolet iS10) and X-ray diffraction (XRD, Advance D8).

2.4. Synthesis of β-CD-CHO. Aldehydic β-CD (β-CD-CHO) was synthesized by the oxidation method. Briefly, 1.4 g β-CD was dissolved in 100 mL water, into which sodium periodate solution (0.6 M, 2 mL) was added dropwise. The pH value of the reactant solution was adjusted by 1.0 M H_2SO_4 to 2.0. After the reaction was stirred for 2 h at room temperature in the dark, 0.3 mL ethylene glycol was then added to inactivate any unreacted periodate. The solution was purified and dried by the abovementioned method. The product was characterized by IR spectra (Nicolet, IS10), and water solubility of the product was detected. Finally, the actual aldehyde content of β-CD-CHO was determined by TNBS assay [23]. Briefly, β-CD-CHO was first reacted with t-BC for 24 h, which was chromogenically reacted with TNBS. The –CHO content was obtained by calculation of absorbance according to a calibration curve, which was constructed from known concentrations of glutaraldehyde solutions (defined CHO groups).

2.5. Preparation of β-CD Functional GO. GO was dispersed in DMSO with a final concentration of 0.5 mg/mL, into which β-CD-CHO was added with a final concentration of 4 mg/mL. The mixture was stirred for 24 h at 40°C, which was further dialyzed with a cutoff molecular weight of 10 k Da and dried by freeze-drying. The product was characterized by infrared spectroscopy (IR, Nicolet iS10) and X-ray diffraction (XRD, Advance D8).

2.6. Characterization of the GO Nanocarrier. The GO nanocarrier was obtained by two-step functionalization. One is FA functionalization to obtain GO-FA; the other was β-CD functionalization to obtain GO-FA-CD. The GO nanocarrier was characterized by transmission electron microscopy (TEM, Tecnai T12).

In vitro drug loading and releasing behaviors were used to evaluate its drug controllable capacity using CPT as a model drug. Different amounts of 1 mg/mL CPT/DMSO solution were added into 10 mL 0.1 mg/mL nanocarrier solution under ultrasonication. Insoluble CPT was separated by a filter and redissolved in ethanol. The remaining CPT was quantified by a spectrophotometric method. Briefly, absorbance at 360 nm of the remaining CPT solution was detected by UV spectroscopy (Cary 50). The loading CPT amount was obtained by calculation of the absorbance by referring to the standard curve.

For CPT release assay, the nanocarrier solution was dialyzed in 10 mL PBS. At appropriate intervals, 2 mL released dialysis solution was withdrawn and the absorbance at 360 nm was recorded to calculate the CPT amount using the same spectrophotometric method. Simultaneously,

3 mL fresh solution was supplemented into dialysis solution. The cumulative CPT release amount was obtained by addition of the remaining CPT amount in the released solution, and the CPT amount was withdrawn each time for detection.

2.7. Statistical Analysis. Data were analyzed using the *t*-test for differences. Results were reported as means ± standard deviation. The significance level was set at $p < 0.05$.

3. Results and Discussion

3.1. Synthesis of FA-MI. In order to expand FA reactivity, maleimide was modified onto FA molecules using the DCC/NHS coupling reaction. $_1$H NMR spectra provided detailed structural information of FA before and after modification, which is shown in Figure 1. The peaks are assigned as follows: peaks from 2.0 to 2.5 ppm and peaks from 4.0 to 4.3 ppm belong to the methane groups of FA, and peaks of 6.9 and 7.5 ppm belong to the -CH=CH- groups of benzene ring on FA molecules, while peaks of 7.7 ppm belong to -CH=CH- of the coupling maleimide unit. The emergence of the maleimide structural unit confirmed the successful grafting of maleimide onto the FA chain.

3.2. Preparation of FA Functional GO. Since dienes could react with dienophile to form a reversible covalent bond, which was the Diels-Alder click chemistry, a maleimide group of FA molecules as a dienophile unit was assumed to react with the diene structure of GO to form FA functional GO. After modification, IR and XRD were used to characterize the results of the reaction in Figure 2. It was found that obvious vibration peaks belonging to amide bands I and II at 1653 cm^{-1} and 1601 cm^{-1} emerged in the IR spectrum of GO-FA sheets besides typical oxide groups on GO sheets like ester groups at 1734 cm^{-1} and 1227 cm^{-1}, aldehyde groups at 1397 cm^{-1}, and the epoxy group at 997 cm^{-1} (Figure 2(a)). Although no definite product structure from the DA click chemistry was found in the IR spectrum of GO-FA, the presence of amide groups also confirmed the successful coupling reaction between GO and FA. From the XRD spectra (Figure 2(b)), the diffraction patterns for GO have mainly one sharp peak at 11°, corresponding to the amorphous form of GO and its sheet thickness. Differently, the peak at 11° after modification was reduced greatly due to a slightly reduced graphene oxide structure, which was also confirmed by a color change of the GO solution from yellowish-brown to dark brown, even black. The reason might be ascribed to autoreduction under a relatively high reaction temperature in the modification process, since the conjugated structure had some characteristics of the reducing agent. If the reaction time is suitable, the modification reaction is also accompanied by the autoreduction reaction. Furthermore, the emergence of peaks at 31° and 45° belonging to the FA crystal structure also confirmed the successful modification of FA on the GO sheet in either chemical coupling or physical interaction.

3.3. Synthesis of β-CD-CHO. β-CD-CHO was obtained by the traditional oxidation method. The IR spectra of β-CD before and after oxidation are shown in Figure 3. The peaks in the β-CD-CHO spectrum are nearly similar to those in the β-CD spectrum except a new small peak at 2850 cm^{-1} belonging to –CHO groups, which indicated the successful oxidation for β-CD. Another evidence for successful modification is the different solubility in water for β-CD and β-CD-CHO in Figure 3. Detailedly, β-CD had good solubility in water, which was witnessed by a homogeneous and transparent β-CD water solution, while equal β-CD-CHO had poorer water solubility than β-CD, which was verified by a white β-CD-CHO dispersion liquid. Furthermore, the CHO content was quantified by TNBS assay, which was about 40% related to the pyranose ring.

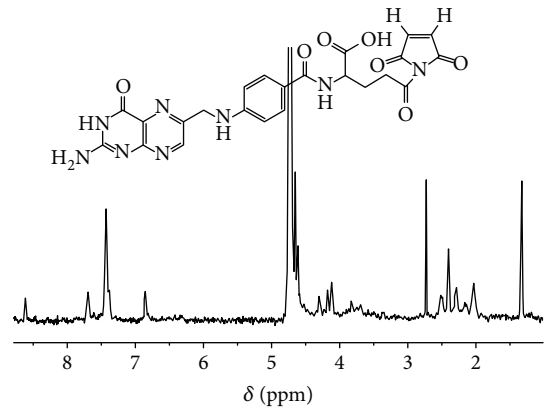

Figure 1: The structure and 1H NMR spectrum of crosslinkable FA.

3.4. Preparation of β-CD Functional GO. In order to test the reactivation of β-CD-CHO, β-CD-CHO was coupled onto GO sheets using a similar method for the preparation of GO-FA. After modification, IR and XRD were used to characterize the results of the reaction in Figure 4. It was found that obvious vibration peaks belonging to ketone groups at 1640 cm^{-1} were shifted and enhanced in the IR spectrum of GO-CD sheets besides typical oxide groups on GO sheets like ester/carboxylic acid groups at 1734 cm^{-1} and 1227 cm^{-1}, aldehyde groups at 1397 cm^{-1}, and the epoxy group at 997 cm^{-1} (Figure 4(a)). Although no specific β-CD structure was found in the IR spectrum of GO-CD, the presence of ketone groups also confirmed the successful coupling reaction between GO and β-CD. From the XRD spectra (Figure 4(b)), the diffraction patterns for GO have mainly one sharp peak at 11°, corresponding to the amorphous form of GO and its sheet thickness. Besides the peak, the emergence of peaks at 21° and 29° belonging to the β-CD crystal structure also confirmed the successful modification of β-CD on the GO sheet in either chemical coupling or physical interaction.

3.5. Characterization of the GO Nanocarrier. Next, the GO nanocarrier was obtained by two-step modification. One was FA modification, and the other was β-CD modification. After modification, the GO nanocarrier exhibited a typical thin wrinkled sheet morphology of GO sheets from the TEM image in Figure 5(a), which indicated that the

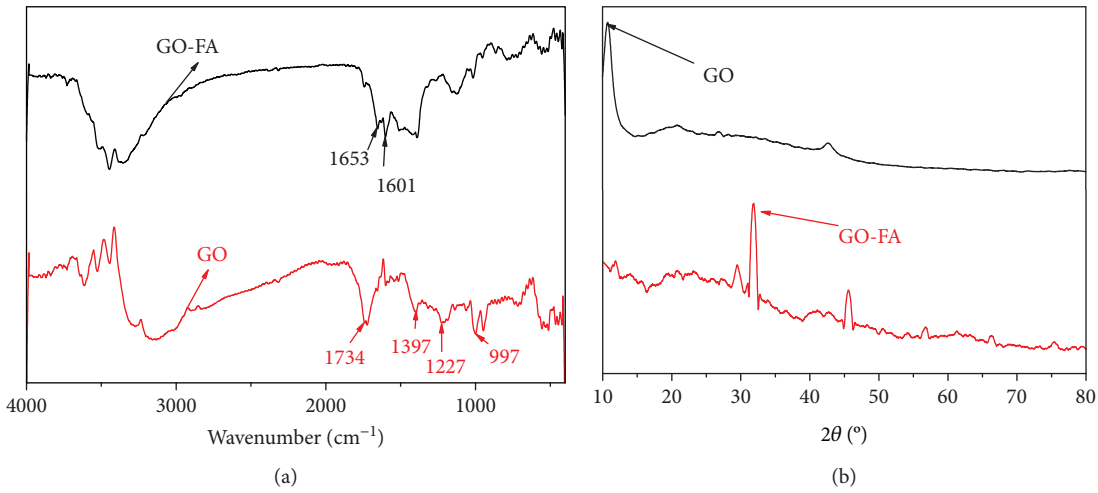

Figure 2: IR spectra (a) and XRD spectra (b) of GO and GO-FA.

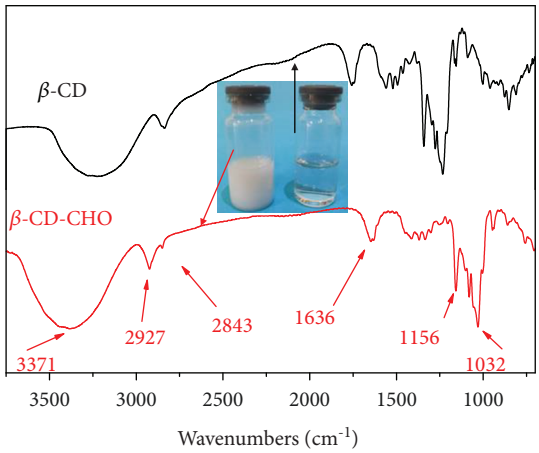

Figure 3: IR spectra of β-CD and β-CD-CHO.

modification had little effect on the morphology. Moreover, the nanocarrier could be stable in either DMSO solution or water solution for one week, which was confirmed by homogeneous nanocarrier solution in Figure 5(b).

The insolubility of CPT in aqueous solution restricted its therapeutic application due to the aqueous physiological environment. Therefore, CPT was usually incorporated into drug carriers to enhance its therapeutic effect, which was loaded onto the GO nanocarrier using a simple mixture and absorbance method in this work. The loaded CPT amount and loaded CPT efficiency as a function of CPT concentration were tracked as shown in Figure 6. The loaded CPT amount increased with the increase in CPT concentration either for unmodified GO sheets or for GO-FA-CD nanocarriers (Figure 6(a)), but the CPT loaded efficiency showed a little decline when the loaded CPT concentration reached 0.2 mg/mL for the GO-FA-CD nanocarrier or the loaded CPT concentration reached 0.1 mg/mL for the GO nanocarrier (Figure 6(b)). More importantly, either the loaded CPT amount or the CPT loaded efficiency for the GO-FA-CD nanocarrier was significantly superior to that for unmodified GO sheets (Figures 6(a) and 6(b)). In one aspect, CPT as a hydrophobic drug could be bound onto GO sheets through $\pi - \pi$ stacking interaction. Therefore, under the action of GO sheets, CPT could be dispersed in the aqueous solution homogenously. In other aspects, CPT could interact with the hydrophobic cavity of β-CD, which could hold more drug molecules. Naturally, the GO-FA-CD nanocarrier had better CPT loading capacity.

In a further step, the CPT release behavior in PBS was tracked as shown in Figure 7. 80% CPT was linearly released from unmodified GO sheets within 4 h, then the remaining 10-20% CPT was gradually released from unmodified GO sheets in the following 56 h. Differently, nearly all CPT was gradually released from the GO nanocarrier within 60 h. Therefore, for CPT release behavior, the GO nanocarrier exhibited better controllability for CPT release, which indicated that modifications would help GO sheets improve its properties as a drug carrier.

Although toxicity of GO as a biomaterial was uncertain according to current research, a number of research confirmed a positive effect of GO on the biomedical field including our own researches. The research provided an available method for its application in the biomedical field.

4. Conclusion

Crosslinkable FA was successfully synthesized by a DCC/NHS coupling reaction, which could be used to modify GO sheets under moderate conditions. IR results confirmed the successful modification of FA onto GO sheets in either chemical coupling or physical interaction. XRD results revealed the crystal structure of FA besides the reduced amorphous structure of GO. Another reactive functional molecule (β-CD-CHO) was synthesized by the simple oxidation method, which was further coupled with GO sheets. IR and XRD results confirmed the successful modification of β-CD-CHO onto GO sheets. Finally, the GO nanocarrier was obtained by two-step modification using the abovementioned methods, which exhibited a typical thin wrinkled sheet morphology of GO sheets without any influence by

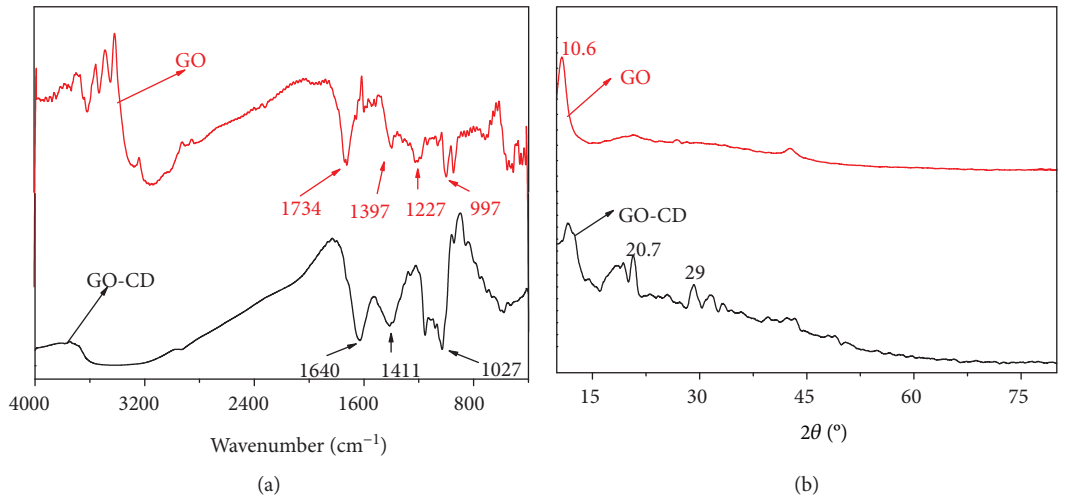

Figure 4: IR spectra (a) and XRD spectra (b) of GO and GO-CD.

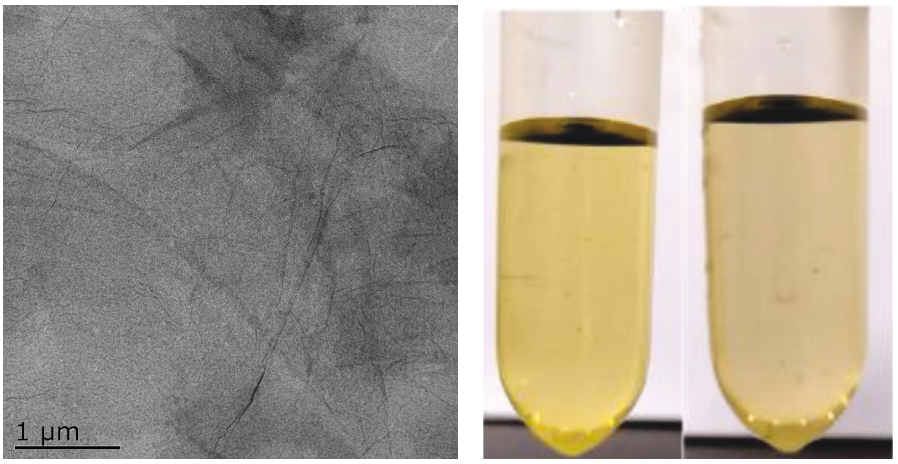

Figure 5: (a) TEM image of GO-FA-CD; (b) nanocarrier solution after being prepared (left) and after being prepared for one week (right).

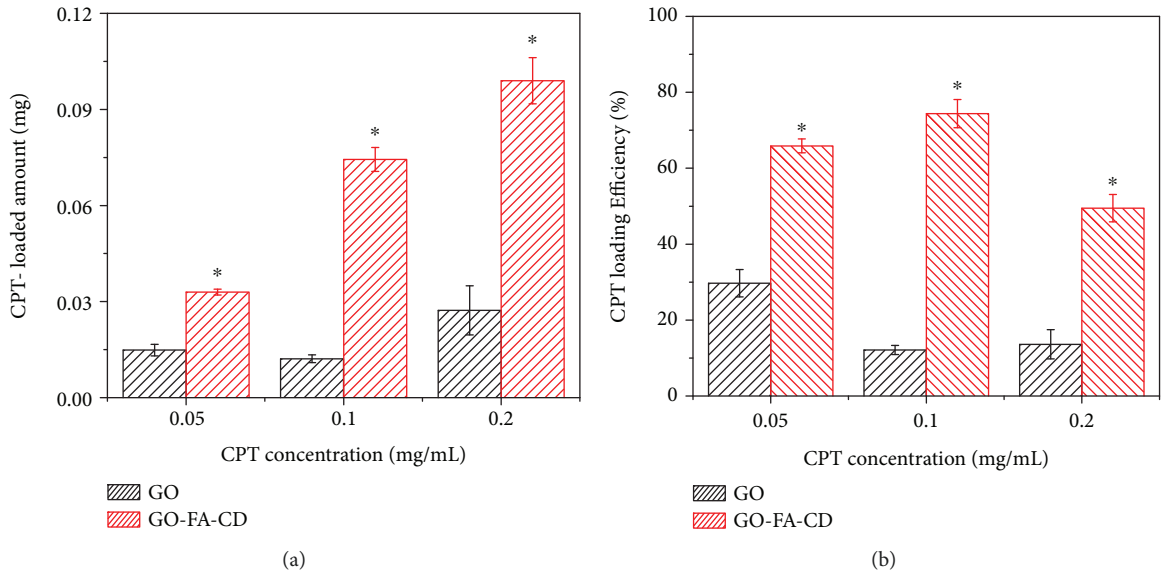

Figure 6: (a) CPT-loaded amount and (b) CPT loading efficiency of GO and GO-FA-CD.

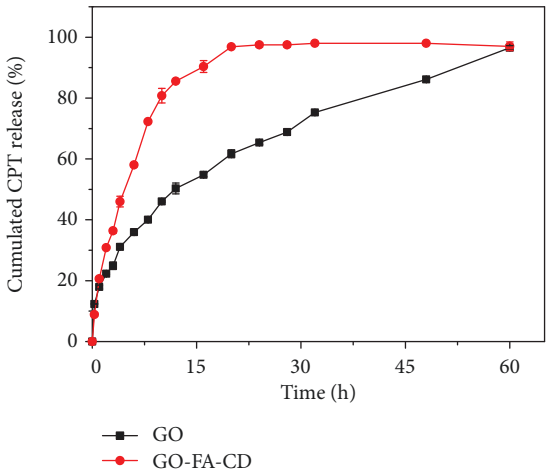

Figure 7: Cumulated CPT release for drug-loaded GO and GO-FA-CD nanocarrier in PBS at 37°C.

two functional molecules. The modifications increased the CPT-loaded amount as well as CPT-loaded efficiency significantly for GO nanocarriers compared with GO sheets. The CPT release behavior revealed that the GO nanocarrier could control CPT release more gently and show better controllability for CPT release.

Data Availability

The data used to support the findings of this study (functional graphene oxide nanocarriers for drug delivery, manuscript 8453493) are included within the article.

Conflicts of Interest

The authors declare that there are no competing interests regarding the publication of this paper.

Acknowledgments

This study is financially supported by the Natural Science Foundation of Jiangsu Province (BK20171113), Qing Lan Project, Six Talent Peaks Project in Jiangsu Province (JY-071), the Excellent Scientific and Technological Innovation team of Jinling Institute of Technology.

References

[1] N. Tyagi, Y. H. Song, and R. De, "Recent progress on biocompatible nanocarrier-based genistein delivery systems in cancer therapy," *Journal of Drug Targeting*, pp. 1–14, 2018.

[2] J. Zhao, Y. Wang, Y. Ma, Y. Liu, B. Yan, and L. Wang, "Smart nanocarrier based on PEGylated hyaluronic acid for deacetyl mycoepoxydience: high stability with enhanced bioavailability and efficiency," *Carbohydrate Polymers*, vol. 203, pp. 356–368, 2019.

[3] S. Banerjee and A. Kundu, "Lipid-drug conjugates: a potential nanocarrier system for oral drug delivery applications," *DARU Journal of Pharmaceutical Sciences*, vol. 26, 2018.

[4] S. Borandeh, A. Abdolmaleki, S. S. Abolmaali, and A. M. Tamaddon, "Synthesis, structural and *in-vitro* characterization of β-cyclodextrin grafted *L*-phenylalanine functionalized graphene oxide nanocomposite: a versatile nanocarrier for pH-sensitive doxorubicin delivery," *Carbohydrate Polymers*, vol. 201, pp. 151–161, 2018.

[5] Y. S. Kim, J. S. Park, M. Park et al., "PLGA nanoparticles with multiple modes are a biologically safe nanocarrier for mammalian development and their offspring," *Biomaterials*, vol. 183, pp. 43–53, 2018.

[6] X. Hu, S. Chen, X. Gong, Z. Gao, X. Wang, and P. Chen, "Synthesis and preparation of biocompatible and pH-responsive cyclodextrin-based nanoparticle," *Journal of Nanoparticle Research*, vol. 19, no. 3, p. 109, 2017.

[7] X. Hu, H. Tan, P. Chen, X. Wang, and J. Pang, "Polymer micelles laden hydrogel contact lenses for ophthalmic drug delivery," *Journal of Nanoscience and Nanotechnology*, vol. 16, no. 6, pp. 5480–5488, 2016.

[8] X. Wang, Z. Gao, L. Zhang, H. Wang, and X. Hu, "A magnetic and pH-sensitive composite nanoparticle for drug delivery," *Journal of Nanomaterials*, vol. 2018, Article ID 1506342, 7 pages, 2018.

[9] Y. Ye and X. Hu, "A pH-sensitive injectable nanoparticle composite hydrogel for anticancer drug delivery," *Journal of Nanomaterials*, vol. 2016, Article ID 9816461, 8 pages, 2016.

[10] Z. Li, L. Tian, J. Liu et al., "Graphene oxide/ag nanoparticles cooperated with simvastatin as a high sensitive X-ray computed tomography imaging agent for diagnosis of renal dysfunctions," *Advanced Healthcare Materials*, vol. 6, no. 18, 2017.

[11] C. Wang, Z. Zhang, B. Chen, L. Gu, Y. Li, and S. Yu, "Design and evaluation of galactosylated chitosan/graphene oxide nanoparticles as a drug delivery system," *Journal of Colloid and Interface Science*, vol. 516, pp. 332–341, 2018.

[12] X. Hu, D. Li, H. Tan, C. Pan, and X. Chen, "Injectable graphene oxide/graphene composite supramolecular hydrogel for delivery of anti-cancer drugs," *Journal of Macromolecular Science, Part A*, vol. 51, no. 4, pp. 378–384, 2014.

[13] X. Hu, X. Ma, H. Tan, and D. Li, "Preparation of water-soluble and biocompatible graphene," *Micro & Nano Letters*, vol. 8, no. 6, pp. 277–279, 2013.

[14] H. Wen, C. Yin, A. Du, L. Deng, Y. He, and L. He, "Folate conjugated PEG-chitosan/graphene oxide nanocomplexes as potential carriers for pH-triggered drug release," *Journal of Controlled Release*, vol. 213, pp. e44–e45, 2015.

[15] V. Kozik, A. Bak, D. Pentak et al., "Derivatives of graphene oxide as potential drug carriers," *Journal of Nanoscience and Nanotechnology*, vol. 19, no. 5, pp. 2489–2492, 2019.

[16] Z. Rao, H. Ge, L. Liu et al., "Carboxymethyl cellulose modified graphene oxide as pH-sensitive drug delivery system," *International Journal of Biological Macromolecules*, vol. 107, Part A, pp. 1184–1192, 2018.

[17] X. J. Kang, Y. L. Dai, P. A. Ma et al., "Poly(acrylic acid)-modified Fe_3O_4 microspheres for magnetic-targeted and pH-triggered anticancer drug delivery," *Chemistry*, vol. 18, no. 49, pp. 15676–15682, 2012.

[18] B. Sahoo, K. S. P. Devi, R. Banerjee, T. K. Maiti, P. Pramanik, and D. Dhara, "Thermal and pH responsive polymer-tethered multifunctional magnetic nanoparticles for targeted delivery of anticancer drug," *ACS Applied Materials & Interfaces*, vol. 5, no. 9, pp. 3884–3893, 2013.

[19] R. I. Pinhassi, Y. G. Assaraf, S. Farber et al., "Arabinogalactan-folic acid-drug conjugate for targeted delivery and target-activated release of anticancer drugs to folate receptor-overexpressing cells," *Biomacromolecules*, vol. 11, no. 1, pp. 294–303, 2010.

[20] S. Chattopadhyay, S. K. Dash, T. Ghosh, D. Das, P. Pramanik, and S. Roy, "Surface modification of cobalt oxide nanoparticles using phosphonomethyl iminodiacetic acid followed by folic acid: a biocompatible vehicle for targeted anticancer drug delivery," *Cancer Nanotechnology*, vol. 4, no. 4-5, pp. 103–116, 2013.

[21] J. Xu, B. Xu, D. Shou, F. Qin, Y. Xu, and Y. Hu, "Characterization and evaluation of a folic acid receptor-targeted cyclodextrin complex as an anticancer drug delivery system," *European Journal of Pharmaceutical Sciences*, vol. 83, pp. 132–142, 2016.

[22] Q. Chen, J. Zheng, X. Yuan, J. Wang, and L. Zhang, "Folic acid grafted and tertiary amino based pH-responsive pentablock polymeric micelles for targeting anticancer drug delivery," *Materials Science and Engineering: C*, vol. 82, pp. 1–9, 2018.

[23] H. Tan, C. R. Chu, K. A. Payne, and K. G. Marra, "Injectable *in situ* forming biodegradable chitosan–hyaluronic acid based hydrogels for cartilage tissue engineering," *Biomaterials*, vol. 30, no. 13, pp. 2499–2506, 2009.